Cell

An O_2-Sensitive Glomus Cell-Stem Cell Synapse Induces Carotid Body Growth in Chronic Hypoxia

Aida Platero-Luengo,[1] Susana González-Granero,[2,3] Rocío Durán,[1] Blanca Díaz-Castro,[1] José I. Piruat,[1] José Manuel García-Verdugo,[2,3] Ricardo Pardal,[1,*] and José López-Barneo[1,3,*]
[1]Departamento de Fisiología Médica y Biofísica, Instituto de Biomedicina de Sevilla (IBiS), Hospital Universitario Virgen del Rocío/CSIC/Universidad de Sevilla, 41013 Seville, Spain
[2]Instituto Cavanilles de Biodiversidad y Biología Evolutiva, Universidad de Valencia, 46071 Valencia, Spain
[3]Centro de Investigación Biomédica en Red sobre Enfermedades Neurodegenerativas (CIBERNED), 28031 Madrid, Spain
*Correspondence: rpardal@us.es (R.P.), lbarneo@us.es (J.L.-B.)
http://dx.doi.org/10.1016/j.cell.2013.12.013

SUMMARY

Neural stem cells (NSCs) exist in germinal centers of the adult brain and in the carotid body (CB), an oxygen-sensing organ that grows under chronic hypoxemia. How stem cell lineage differentiation into mature glomus cells is coupled with changes in physiological demand is poorly understood. Here, we show that hypoxia does not affect CB NSC proliferation directly. Rather, mature glomus cells expressing endothelin-1, the O_2-sensing elements in the CB that secrete neurotransmitters in response to hypoxia, establish abundant synaptic-like contacts with stem cells, which express endothelin receptors, and instruct their growth. Inhibition of glomus cell transmitter release or their selective destruction markedly diminishes CB cell growth during hypoxia, showing that CB NSCs are under the direct "synaptic" control of the mature O_2-sensitive cells. Thus, glomus cells not only acutely activate the respiratory center but also induce NSC-dependent CB hypertrophy necessary for acclimatization to chronic hypoxemia.

INTRODUCTION

Adult stem cells reside within specific "niches" that provide the appropriate environment to maintain their ability for self-renewal and multipotency. These cells are normally in a dormant state that protects them from stressors; the manner by which they are selectively activated to progress from quiescence to differentiated mature cells is still to be resolved (Suda et al., 2011; Chell and Frisén, 2012). Neural stem cells (NSCs), which resemble embryonic radial glia-like cells and are able to generate new neurons and glial cells, persist in two niches in the adult mammalian central nervous system (CNS): the subventricular zone (SVZ) and the subgranular layer of the hippocampus (SGZ) (Álvarez-Buylla and Lim, 2004; Zhao et al., 2008). Central neurogenesis is crucial for numerous brain functions, and its impairment could be involved in some neuropsychiatric disorders (Kriegstein and Álvarez-Buylla, 2009; Ming and Song, 2011). NSCs can sense neuronal activity as a result of which adult neurogenesis is modulated by experience and environmental stimuli. However, the coupling of lineage progression to physiological demand remains poorly understood. Several neurotransmitters modulate neurogenesis, one well-known example being the inhibition of SVZ cell proliferation in animals with dopaminergic nigrostriatal denervation (Höglinger et al., 2004). Transmitter "spill-over" from neighboring GABA-producing SVZ neuroblasts has been shown to provide an inhibitory feedback input for NSC proliferation (Liu et al., 2005; Ge et al., 2006). Moreover, glutamate (Deisseroth et al., 2004) and GABA (Tozuka et al., 2005) released from the hippocampal circuitry can modulate neural progenitors in the SGZ and induce neuronal differentiation. Recently, a mature granule cell to NSC connection, mediated by hippocampal GABAergic interneurons, was shown to couple neuronal activity to neurogenesis in the SGZ (Song et al., 2012).

Multipotent NSCs of glial lineage also exist in the adult carotid body (CB), a neural crest-derived paired organ located in the carotid bifurcation (Pardal et al., 2007). The CB is composed of clusters (glomeruli) of neuron-like glomus (type I) cells that are electrically excitable and have numerous secretory vesicles containing neurotransmitters and neuropeptides. Glomus cells are surrounded by processes of glia-like sustentacular (type II) cells. This organ is the main arterial chemoreceptor that mediates reflex hyperventilation during hypoxemia. Glomus cells, the primary O_2-sensing elements in the CB, depolarize in response to hypoxia, thereby releasing neurotransmitters that activate sensory nerve fibers terminating in the brainstem respiratory center (see López-Barneo et al., 2001). In addition to this fundamental role in acute oxygen sensing, the CB exhibits a remarkable structural plasticity that is uncommon for a neural tissue, which is manifested upon chronic exposure to hypoxia. The CB grows to several times its normal size during acclimatization in high-altitude dwellers (Arias-Stella and Valcarcel, 1976) or in hypoxemic patients suffering cardiopulmonary disorders (Heath et al., 1982). We have shown that the glia-like type II cells, selectively

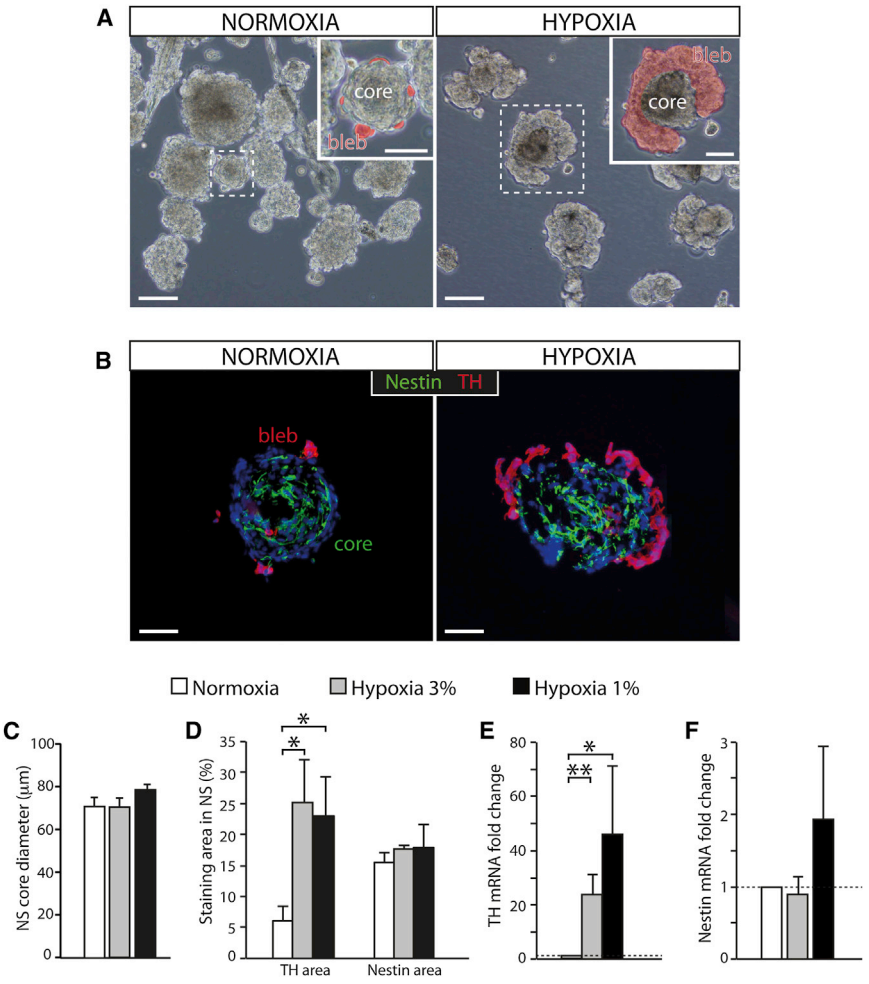

Figure 1. Differential Effects of Hypoxia on CB NSC Proliferation and Differentiation

(A) Bright-field images of CB primary neurospheres (NS) cultured under normoxia (Nx, 21% O_2) or hypoxia (Hx, 3% O_2). Differentiating blebs are pseudocolored in red in the insets. Scale bars, 100 μm (50 μm in insets).

(B) CB NS composed of a core of nestin+ progenitors and blebs of TH+ cells as revealed by immunofluorescence. Scale bars, 50 μm.

(C) Quantification of NS core diameter in cultures grown at different levels of hypoxia (six cultures for Nx and Hx 3% O_2 and 3 cultures for Hx 1% O_2).

(D) Quantification of nestin+ or TH+ staining area in normoxic and hypoxic NS sections. Note that the TH+ area clearly increased under Hx, whereas the nestin+ area did not change (n = 4 independent cultures).

(E and F) qPCR results showing relative expression of TH and nestin in NS at different levels of O_2 tension. The expression of TH significantly increased under hypoxia, whereas nestin expression showed a nonsignificant variability (n = 7 cultures in Nx and Hx 3% O_2; 4 cultures for Hx 1% O_2). In (C)–(F), error bars are SEM. *p < 0.05 and **p < 0.01.

See also Table S1.

expressing glial fibrillary acidic protein (GFAP), are NSCs and contribute to CB growth in hypoxia. These cells form clonal colonies in vitro that are enriched in proliferating nestin-positive(+) progenitors that give rise to mature glomus cells and other neural crest cell lineages. Similarly, cell fate experiments in vivo have demonstrated that NSCs contribute to the generation of new glomus cells in animals exposed to sustained hypoxia (Pardal et al., 2007).

Stem cells in the CB neurogenic center are quiescent under normoxic conditions. Nonetheless, they become activated upon lowering blood O_2 tension (hypoxia), a well-defined and controllable variable. Therefore, the CB niche provides an ideal model in which to study activity-dependent neurogenesis and to explore the mechanisms whereby stem cells switch from dormancy to cycling. Herein, we show that, unexpectedly, CB NSC proliferation in vitro is insensitive to hypoxia over a broad range of O_2 tensions. We provide compelling structural and functional evidence supporting the existence of abundant direct "synaptic" contacts between mature neuron-like, O_2-sensitive, glomus cells and glia-like progenitors, thus optimizing the activity-dependent stimulation of stem cells. The release of stored neurotransmitters from glomus cells during hypoxia induces proliferation of progenitor cells and growth of the CB. Among the substances released by glomus cells, we have identified endothelin-1 (ET-1), an agent involved in neural crest progenitor specification and migration (Shin et al., 1999; Bonano et al., 2008), as a powerful activator of CB stem cell proliferation in vitro and in vivo. In this way, O_2-sensing glomus cells mediate both the acute activation of the respiratory center and the chronic induction of CB growth upon exposure to hypoxia.

RESULTS

Contrasting Effects of Hypoxia on CB Stem Cell Proliferation and Dopaminergic Differentiation

CB stem cells cultured in floating conditions generate neurospheres composed of an initial cell mass (core) containing numerous proliferating nestin+ intermediate neural progenitors. The neurosphere core grows in size with time in culture, thereby providing an estimation of progenitor proliferation. After several days, the core is surrounded by peripheral blebs of differentiated dopaminergic, tyrosine hydroxylase (TH)-positive(+) glomus cells (Pardal et al., 2007) (Figures 1A and 1B). As hypoxia is the signal that triggers CB growth, we tested whether lowering the O_2 tension increased the proliferation of CB progenitors (Kokovay and Temple, 2007). Somewhat surprisingly, decreasing O_2 tension (in the range between 21% and 1%) did not alter the diameter of the neurosphere core measured 10 days after plating (Figures 1A–1C). This finding was confirmed by estimating the

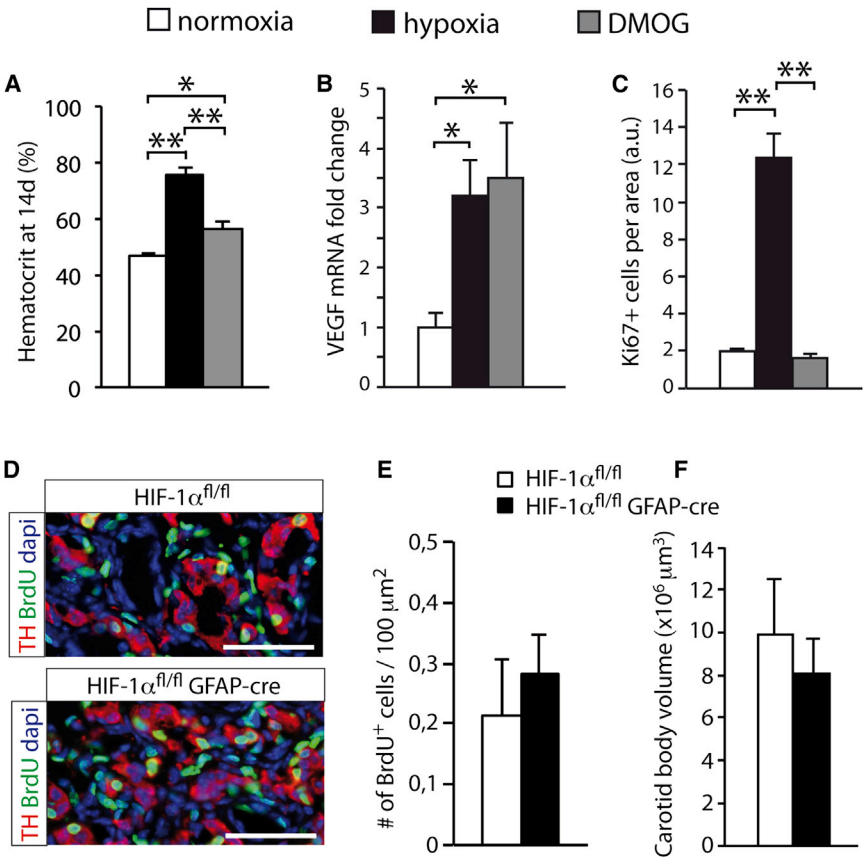

Figure 2. HIF Stabilization Does Not Induce CB Growth

(A) Quantification of the hematocrit in rats exposed to hypoxia (10% O_2) or maintained in a normal atmosphere and treated with DMOG for 14 days, in comparison with normoxic rats. Note that inhibition of prolyl hydroxylases with DMOG increased the hematocrit, although to a lesser extent than hypoxia.

(B) Quantitative PCR showing the overexpression of VEGF, an HIF-dependent gene, in the brain of rats exposed to Nx, Hx, or treated with DMOG.

(C) Quantification of the density of Ki67+ cells within the CB parenchyma of rats exposed to Nx (21% O_2), Hx (10% O_2), or DMOG (21% O_2) for 3 days. DMOG did not increase cell proliferation in the CB despite inducing HIF-dependent genes (three rats per group). In (A)–(C), error bars represent SEM. *$p < 0.05$ and **$p < 0.01$.

(D) Immunohistochemistry of BrdU and TH in CBs of HIF-1$\alpha^{fl/fl}$ GFAP-cre and WT mice exposed to Hx 10% O_2 for 19 days. Scale bars, 50 μm.

(E and F) BrdU+ cell number (E) and CB volume (F) in HIF-1$\alpha^{fl/fl}$ GFAP-cre and WT mice exposed to chronic Hx (five CBs from three mutant mice and three CBs from two WT mice). In (E) and (F), error bars represent SEM.

See also Table S1.

area of nestin+ cells (Figure 1D) or the level of nestin mRNA (Figure 1F) in the neurospheres. In contrast, the size of the TH+ blebs (Figures 1A, 1B, and 1D) and TH mRNA level (Figure 1E) markedly increased during exposure to hypoxia. These results indicate that proliferation of CB NSCs is not directly regulated by hypoxia, even when these cells are exposed to O_2 tensions as low as 1% O_2, a level far below that necessary to evoke acute secretory responses in glomus cells (Ortega-Sáenz et al., 2010). As in other cell types (Czyzyk-Krzeska et al., 1992), hypoxia upregulated TH mRNA and favored dopaminergic differentiation of CB NSCs, similar to what has been described in sympathoadrenal progenitors (Morrison et al., 2000).

Systemic Inhibition of Prolyl Hydroxylases Does Not Induce Proliferation of CB Cells

In parallel with the in vitro experiments, we also tested whether mimicking hypoxia by inhibition of prolyl hydroxylases (PHDs) with dimethyloxalylglycine (DMOG) induced CB NSC proliferation in vivo. PHDs are O_2-sensitive enzymes whose inhibition by the lack of O_2 permits stabilization of hypoxia-inducible factors (HIFs), which in turn regulate the expression of a broad variety of O_2-sensitive genes, some of which are involved in cell proliferation (Kaelin and Ratcliffe, 2008). Similar to chronic hypoxia, application of DMOG for several days resulted in the induction of HIF-dependent genes such as those for erythropoietin to increase the hematocrit (Figure 2A) and brain vascular endothelial growth factor (VEGF; Figure 2B). However, in contrast with hypoxia, DMOG treatment was unable to produce an appreciable proliferation of CB cells (Figure 2C). Hypoxic CB cell proliferation and organ growth were also normal in animals with ablation of HIF-1α in GFAP-positive cells (Figures 2D–2F). These data suggest that neither activation of the HIF pathway nor HIF-1α inhibition is the primary signal that triggers cell proliferation and CB growth in hypoxic conditions.

Structure of Glomus Cell-Type II Cell "Synapses"

We hypothesized that hypoxia-dependent CB progenitor proliferation in situ could take place secondarily to the activation of mature glomus cells, which show hypoxia-evoked quantal transmitter release that is unaffected by DMOG but is exquisitely dependent on the level of O_2 tension (Ortega-Sáenz et al., 2007; Ortega-Sáenz et al., 2010). This idea fits well with the close structural relationship that exists between TH+ type I cells and GFAP+ type II cells, which are quiescent progenitor cells (Pardal et al., 2007). Indeed, as reported in numerous electron microscope (EM) studies, large surface areas of type I cells are actually enveloped by the processes of type II cells (Figure 3A). Here, we performed EM analyses to study these type I-type II cell contacts and found that the two cell types were clearly distinguishable in ultrathin sections. In this way, glomus cells have a large cytoplasmic domain containing abundant mitochondria, long endoplasmic reticulum cisternae, and, in particular, numerous secretory vesicles (Figures 3A and 3B). It is known that glomus cells function as presynaptic-like elements, which, in response to hypoxia, acutely release vesicle-stored neurotransmitters in

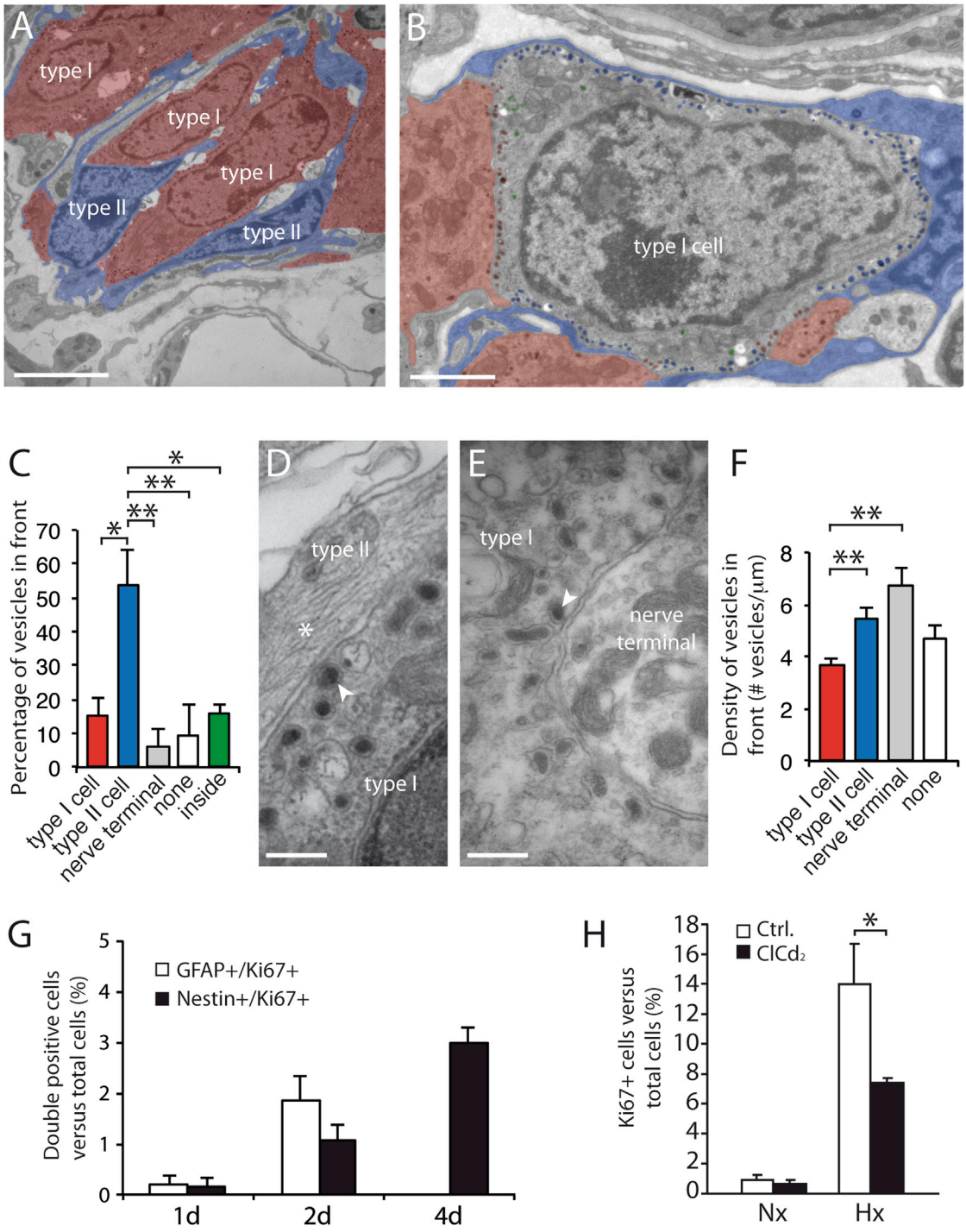

Figure 3. Synaptic-like Contacts between Neuron-like Type I and Glia-like Type II Cells within the CB Parenchyma

(A) Pseudocolored electron micrograph of a CB ultrathin section of a normoxic animal showing the close association of type II progenitor cells with type I neuronal cells. Scale bar, 5 μm.

(B) Pseudocolored electron micrograph illustrating the cellular elements surrounding a typical type I cell within the CB parenchyma. Type II cells and the type I vesicles facing them appear in blue; type I cells and the vesicles facing them appear in red; vesicles away from the membrane (inside in C) appear in green. Scale bar, 2 μm.

(C) Quantification of the percentage of type I dense-core vesicles facing each of the different cellular elements surrounding a typical type I cell.

(D and E) Electron micrographs of a CB showing details of the contact area between type II and type I cells (D) or between a type I and a nerve terminal (E). Examples of exocytotic vesicles apposed near the membrane are indicated with arrowheads. A bundle of intermediate filaments, characteristic of type II cells, is indicated by an asterisk in (D). Scale bars, 0.2 μm.

(legend continued on next page)

an external Ca^{2+}-dependent manner, thereby activating afferent chemosensory fibers (Ureña et al., 1994; Buttigieg and Nurse, 2004). However, an intriguing property of glomus cells is that their secretory vesicles do not seem to be clustered facing nerve terminals but are more uniformly distributed over the entire glomus cell surface (Figure 3B). Indeed, a quantitative analysis of the number of vesicles located in front of the various cell membranes surrounding glomus cells showed that the vast majority of vesicles lay near type II cells (Figure 3C). Even the density of secretory granules in the different glomus cell "presynaptic" regions was the same when the "postsynaptic" membrane was either a nerve terminal or a type II cell (Figures 3D–3F). Often, the glomus cell membrane (with submembranous localization of dense-core vesicles) was separated from a type II cell by <50 nm (Figure 3D), which is similar to the space in glomus cell-nerve terminal synapses (Figure 3E). "Synaptic" contacts between neighboring type I cells were also frequently observed (Figures 3B and 3C). Therefore, it is likely that the transmitters released from "presynaptic" glomus cells in response to hypoxia not only activate the afferent sensory fibers but could also bind to receptors and modify the function of "postsynaptic" type II and/or type I cells. These observations strongly suggest that O_2-sensing glomus cells are essential for triggering the proliferation of CB progenitor cells in hypoxia.

CB Growth in Hypoxia Requires Activation of Glomus Cells

The time course of CB cell proliferation induced by hypoxia in vivo is illustrated in Figures 3G and 3H. Animals were maintained in a 10% O_2 atmosphere for variable time periods and, after CB removal, proliferating cells were identified based on their expression of Ki67. Within this population, we also identified cells coexpressing selective markers: type II cells (GFAP+), intermediate progenitors (nestin+), type I cells (TH+), and endothelial cells (lectin+) (Figure S1A available online). The number of proliferating progenitor (GFAP+ or nestin+) cells increased during the days following exposure to hypoxia. Proliferation of lectin+ endothelial cells was only observed at later stages of hypoxia (data not shown). Initially, numerous cells were GFAP+ (indicating proliferation of stem cells) but, as previously reported (Pardal et al., 2007), this phenotype disappeared a few days after exposure to hypoxia in parallel with the appearance of nestin+ intermediate progenitors (Figure 3G). In addition to the CB progenitors, the Ki67 marker also labeled a significant number of proliferating TH^+ cells (see Discussion). Glomus cells respond to hypoxia with a rise in cytosolic Ca^{2+} and a quantal release of transmitters that is inhibited in vitro by blockade of Ca^{2+} channels with Cd^{2+} and other divalent cations (Ureña et al., 1994; Buttigieg and Nurse, 2004). In line with this observation, systemic administration of subtoxic doses of Cd^{2+} (Stosic et al., 2010) to animals exposed to hypoxia resulted in a marked reduction in the number of Ki67+ CB cells (Figure 3H). Other highly proliferative tissues, such as the gut epithelium, remained unaffected by the systemic administration of Cd^{2+}, thus ruling out the possibility of a toxic effect (data not shown).

Further support for the essential role played by glomus cells in triggering CB growth in hypoxia was obtained from experiments performed on TH-SDHD mice. These animals lack the "D" subunit of mitochondrial complex II in TH+ cells and show a marked loss of catecholaminergic cells in the CB and other tissues (Díaz-Castro et al., 2012). A detailed EM analysis of the CB from TH-SDHD mice indicated marked disruption of the CB glomeruli (Figures 4A and 4B), with type I (glomus) cells in different stages of degeneration displaying increased numbers of mitochondria (which were dilated and had disorganized cristae) and the appearance of numerous vacuoles (Figures 4C and 4D). The number of dense-core secretory vesicles, a typical feature of glomus cells (Figures 4C and 4E), was markedly reduced in the TH-SDHD mice (Figures 4D and 4F). As the gene mutation in this model is restricted to glomus cells, type II cells appeared normal, showing their typical ultrastructural characteristics: fusiform nucleus, large nucleolus, scarce perinuclear cytoplasm with few mitochondria, and the absence of secretory vesicles. They also displayed the characteristic long processes enveloping type I cells (Figures 4A, 4B, 4G, and 4H). Dissociated cells from CBs of the TH-SDHD mice were able to form neurospheres in vitro, further supporting the conclusion that the function of type II cells was unaltered in these animals. TH-SDHD mice are normal in normoxia but die within hours/days after exposure to 10% O_2 tension, probably because the lack of a functional CB renders them unable to acclimatize to sustained hypoxia (see Discussion). However, these animals survived in 14% O_2 tension for more than a week. The proliferation of CB progenitor cells, induced after 6 days in a 14% O_2 atmosphere, was clearly reduced in TH-SDHD mice compared with wild-type (WT) animals (Figures 4I and 4J). Taken together, the experiments performed with Ca^{2+} channel blockers (that decrease transmitter release from O_2-sensitive glomus cells), as well as those carried out in CBs with damaged and vesicle-depleted glomus cells (TH-SDHD mice), strongly suggest that activation of glomus cells is the initial step inducing CB growth upon exposure to hypoxia.

Endothelin-1 Synthesized and Released by Glomus Cells Regulates Cell Proliferation and CB Growth

Among the various transmitters and neuropeptides existing in the CB, we focused our study on endothelin-1 (ET-1) because this peptide and endothelin receptor A (ET-RA) are abundant in glomus cells (McQueen et al., 1995; Paciga et al., 1999; Chen et al., 2002). Moreover, G-protein-coupled endothelin receptors

(F) Quantification of the density of type I dense-core vesicles per unit length of glomus cell membrane depending on the cellular element present in front. The density was significantly higher when a type II cell or a nerve terminal appeared as "postsynaptic" membrane; $^{**}p < 0.01$.

(G) Quantification of proliferating CB progenitor cells after removal of the organ and dissociation of the cells during the initial days after exposure to hypoxia (three rats per group).

(H) Quantification of proliferative cells (Ki67+) among the total cell population from dissociated CBs of rats exposed to 2 days of Nx (six rats) or Hx (seven rats), with or without intraperitoneal injection of cadmium; $^{*}p < 0.05$.

In (C), (F), (G), and (H), error bars represent SEM. See also Figure S1A.

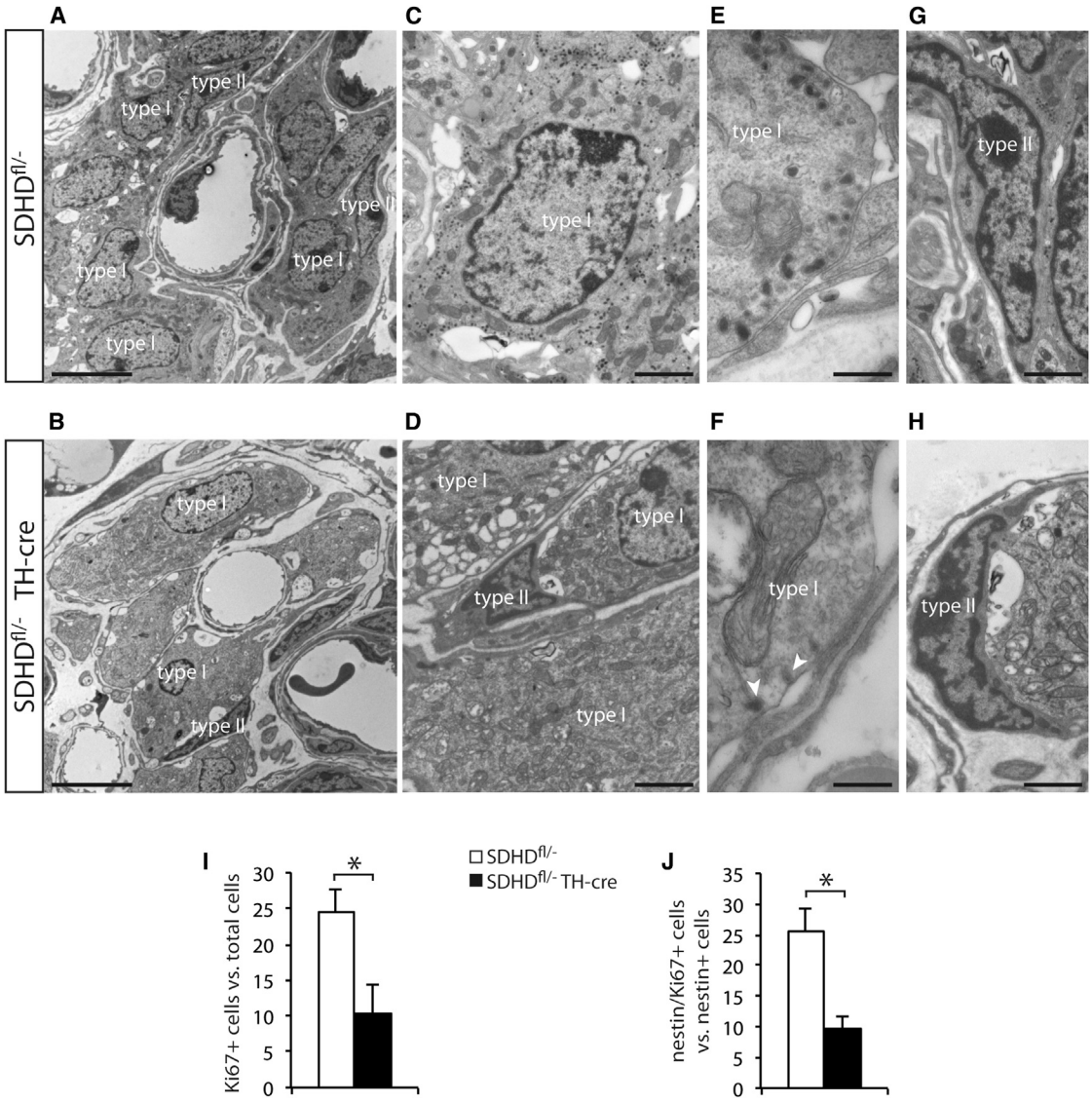

Figure 4. Genetic Disruption of Type I Cell Function Diminishes CB Proliferative Activation under Hypoxia

(A) Electron micrograph showing the CB neural parenchyma of an SDHD$^{fl/-}$ (control) mouse to illustrate the normal appearance of type I and type II cells. Scale bar, 5 μm.

(B) Electron micrograph showing the CB neural parenchyma of an SDHD$^{fl/-}$ TH-cre mutant mouse to illustrate the abnormal appearance of type I cells with smaller nuclei and enlarged cytoplasm. Scale bar, 5 μm.

(C) Detail of a type I cell in the CB of a control mouse containing numerous dense-core vesicles. Scale bar, 2 μm.

(D) Detail of CB type I cells in a mutant mouse. Cells show an increased number of mitochondria and almost no dense-core vesicles. The type I cell at the top left also has numerous vacuoles. Scale bar, 2 μm.

(E) Detail of dense-core vesicles within the cytoplasm of a type I cell in the CB of a control mouse. Scale bar, 0.5 μm.

(F) Detail of the cytoplasm of a type I cell in the CB of an SDHD$^{fl/-}$ TH-cre mouse, in which mitochondrial dysfunction resulted in a marked decrease in the number of secretory vesicles. Arrowheads indicate two vesicles present in this field. Scale bar, 0.5 μm.

(G) Detail of a typical type II cell in the CB neural parenchyma of a control mouse. Scale bar, 2 μm.

(H) Normal disposition and appearance of a type II cell surrounding a type I cell in the CB neural parenchyma of an SDHD$^{fl/-}$ TH-cre mouse. Scale bar, 2 μm.

(I and J) Quantification of Ki67+ (I) or nestin/Ki67 double-positive (J) cells versus total dissociated cells from the CBs of SDHD$^{fl/-}$ (n = 4) or SDHD$^{fl/-}$ TH-cre (n = 3) mice exposed to Hx 14% O_2 for 6 days.

Error bars represent SEM. *p < 0.05.

(A and B) mediate cell proliferation in several tissues (Koyama and Michinaga, 2012) and are required for the correct specification (Bonano et al., 2008) and migration (Shin et al., 1999) of neural crest progenitors. The CB is profusely irrigated, and as a result, unequivocal identification of ET-1 in glomus cells is hampered by the presence of abundant endothelial cells that

highly express ET-1 (see Rubanyi and Polokoff, 1994 and Figures S1B and S1C). Indeed, a large percentage of cells dissociated from the CB were sorted with the specific endothelial cell marker CD31 (Figure 5A). As expected, this TH− and cadherin-5+ (another endothelial cell marker) population contained a significant amount of ET-1 mRNA (Figure 5B). However, ET-1 mRNA was also highly expressed in the CD31− population, which includes TH+ glomus cells (Figure 5B). As in other tissues (Elton et al., 1992), ET-1 mRNA was upregulated by hypoxia in dissociated CB cells maintained in vitro (Figure 5C). The CD31+ population completely disappeared in CB-derived neurospheres (Figures 5D and 5E). However, these preparations expressed high levels of ET-1 mRNA, which was also markedly induced by hypoxia (Figure 5F). ET-1 expression was particularly high in differentiated neurospheres, enriched in TH+ cells (insets in Figures 5D–5F and S2). Definitive support for the localization of ET-1 in glomus cells was obtained from experiments performed on TH-EGFP mice, which allowed us to sort a pure population of ET-1-expressing glomus cells (Figures 5G and 5H).

There are two main types of endothelin receptor: ET-RA and ET-RB (Hosoda et al., 1994; Clouthier et al., 1998). We detected abundant ET-RA and ET-RB mRNAs in both CB tissue and CB-derived neurospheres (Figure 6A). The presence of ET-RA and ET-RB in TH+ glomus cells, as well as in TH− type II cells, was also evidenced by immunohistochemistry (Figures 6B and 6C). ET-RA was more abundantly expressed in the CB (~40% of the cells) than ET-RB (~20% of the cells). However, whereas ET-RB was highly expressed in all GFAP+ or nestin+ cells (see Figures 6D and 6E), ET-RA was only weakly expressed in ~40% and 7% of GFAP+ or nestin+ cells, respectively. In contrast, ET-RA appeared in all TH+ cells. Interestingly, <3% of TH+ cells expressed ET-RB, and the quantitative analysis of ET-RB mRNA expression clearly showed that it is far more abundant in undifferentiated than in differentiated neurospheres (Figure 6F). These observations indicate that, whereas ET-1 synthesis is induced in glomus cells during hypoxia, endothelin receptors (particularly ET-RB) are highly expressed in stem cells and proliferating CB progenitor cells, thereby suggesting an ET-1-mediated communication between mature glomus cells and stem cells. In line with this concept and previous reports (Chen et al., 2007), bosentan, a nonselective endothelin receptor antagonist used as an antiproliferative drug, inhibited CB cell proliferation during exposure to hypoxia (Figures 6G and S3).

The effect of ET-1 on CB cell proliferation was directly demonstrated in vitro (Figure 7A). ET-1 added to CB cell cultures increased neurosphere-forming efficiency (Figure 7B), neurosphere core diameter, and the number of nestin+ cells (Figures 7C and 7D) in a dose-dependent manner (Figure 7E). As observed in vivo, CB progenitor proliferation induced by ET-1 was inhibited by the presence of an endothelin receptor antagonist (Figure 7F). In parallel with the increase in progenitor proliferation, there was an ET-1-mediated decline in differentiation to TH+ glomus cells (Figure S4). The pharmacological effects of ET-1 and endothelin receptor blockade were further confirmed by experiments in which receptor expression was selectively downregulated by specific siRNAs (Figures S5A and S5B). This did not interfere with the neurosphere growth but reduced by almost 50% the stimulatory effect of ET-1 on neurosphere core diameter (Figures 7G and S5C). Binding of ET-1 to its receptors leads to activation of the MAP kinase signaling pathway with induction of *c-myc* and other proproliferative and antiapoptotic genes (Wang et al., 1994; Shichiri et al., 1998). This characteristic response to ET-1 was also observed in CB neurosphere cultures (Figure 7H). ET-1 increased the expression of the Ki67 proliferation marker in nestin+ progenitor cells (Figure S6), confirming a direct induction of CB NSC proliferation.

DISCUSSION

CB Neural Stem Cell Activation Is Not Directly Regulated by Hypoxia

O_2 tension has been recognized as an important variable that regulates self-renewal, proliferation, and differentiation of stem cells (Panchision, 2009; Mohyeldin et al., 2010). Most adult stem cell niches have a relatively low O_2 tension that helps to maintain the cells in a dormant state with predominantly anaerobic metabolism, preserving them from excessive production of reactive oxygen species and other stressors (Suda et al., 2011). In normoxia, CB stem cells also appear to be quiescent (Pardal et al., 2007). Nonetheless, we expected that hypoxia could directly modulate the proliferative status of the stem cells to induce growth of the organ. Stabilization of HIF has been reported to induce proliferation in several cell types (Kaelin and Ratcliffe, 2008), including hippocampal NSCs (Panchision, 2009; Suda et al., 2011). Somewhat surprisingly, chronic exposure of CB stem cells in vitro to hypoxia did not affect proliferation of progenitors in the neurospheres. These findings were in fair agreement with in vivo experiments showing that inhibition of O_2-sensitive PHDs with DMOG did not evoke CB growth or progenitor proliferation. Similar results in vivo have been obtained independently using a different PHD inhibitor (Bishop et al., 2013). Our data indicate that HIF activation or HIF-1α inhibition are not the primary signals that trigger the transition of CB NSCs from quiescence (in normoxia) to proliferation (in hypoxia). They also suggest that physiological activation of CB progenitors by hypoxia is a niche property rather than an intrinsic characteristic of the stem cells.

Oxygen-Dependent Activation of the CB Niche Is Mediated by Direct Neuronal-Stem Cell Chemical Synapses

A fundamental question under intense scrutiny is how stem cells in the niches progress from quiescence to proliferation, allowing them to respond to the dynamic needs of tissues (see Chell and Frisén, 2012). Puzzled by the finding that CB NSC proliferation is unaffected by hypoxia, we hypothesized that mature glomus cells, acting as acutely responding O_2 sensors (see López-Barneo et al., 2001), could induce type II cell activation during exposure to low PO_2. We have found compelling structural evidence indicating that most of the secretory vesicles in glomus cells are actually located facing type II cells. Glomus and type II cells are frequently separated by a "synaptic space" (<50 nm) similar to that existing between glomus cells and nerve terminals. Therefore, as well as the effect on the chemosensory synapse activating the respiratory center, neurotransmitter release from

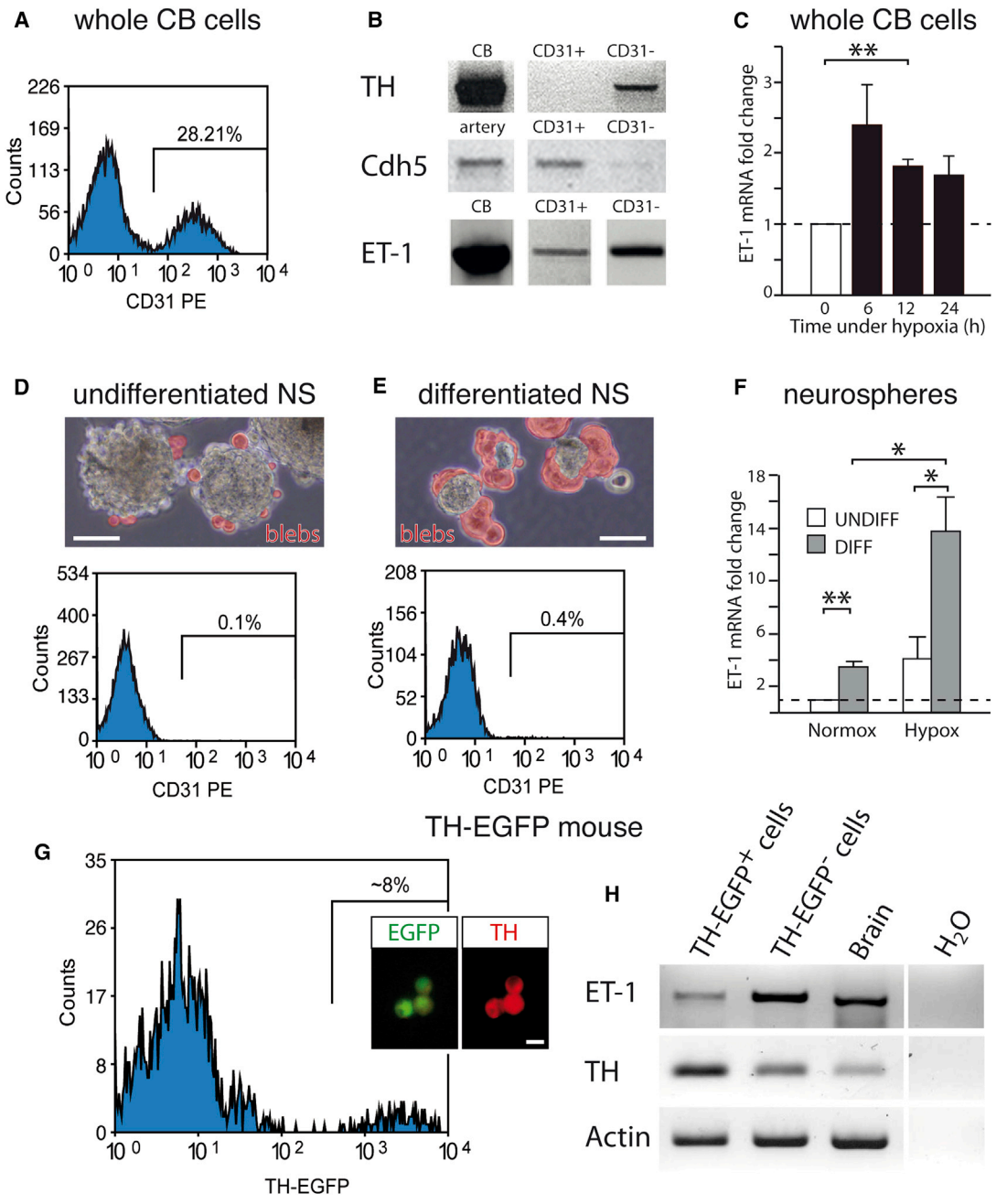

Figure 5. ET-1 Expression in CB Glomus Cells In Vivo and In Vitro

(A) Flow cytometry histogram of dissociated whole CB cells stained with CD31.

(B) Nonquantitative PCR showing the expression of TH, cadherin 5 (Cdh5), and ET-1 in different cell populations sorted from dissociated CB preparations by flow cytometry.

(C) Quantitative PCR data illustrating the induction of ET-1 expression in CB cells exposed to chronic hypoxia (1% O_2) for the indicated periods (n = 5 cultures).

(D and E) Top, bright-field pictures of undifferentiated and differentiated NS, with differentiated blebs pseudocolored in red. Bottom, flow cytometry histograms showing the absence of CD31+ endothelial cells in both types of NS. Scale bars, 50 μm.

(F) Quantitative PCR showing the higher expression of ET-1 in differentiated (enriched for TH^+ cells) in comparison with undifferentiated NS after 2 days in normoxic or hypoxic (1% O_2) culture conditions (n = 3 different cultures per condition). In (C) and (F), error bars represent SEM. *$p < 0.05$ and **$p < 0.01$.

(G) Flow cytometry histogram of dissociated CB cells from TH-EGFP mice. The inset shows immunocytochemistry results illustrating that all EGFP+ cells sorted were TH+ (over 100 cells checked). Scale bar, 10 μm.

(H) PCR analysis showing ET-1 expression in sorted TH+ cells. PCR bands are shown separated from each other (B and H) when superfluous lanes have been removed from the gel.

See also Figures S1B, S1C, S2, and Table S1.

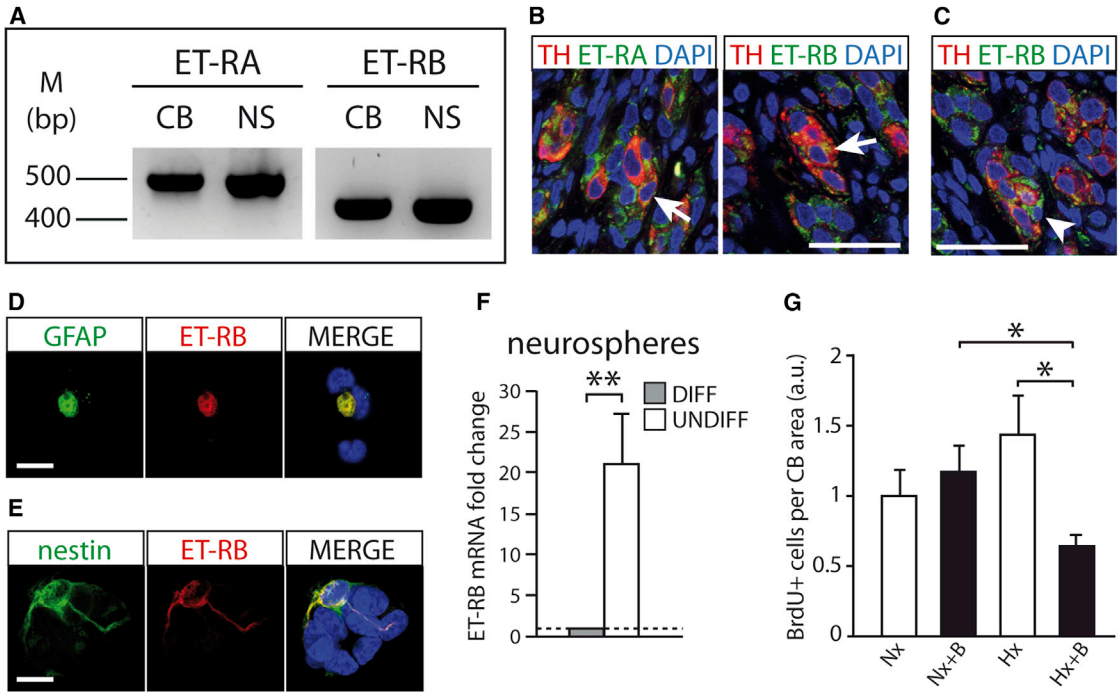

Figure 6. ET-1 Receptor Expression in CB Parenchyma and Effects of ET-1 on CB Growth

(A) Nonquantitative PCR revealing expression of endothelin receptors A and B in whole CB and NS.

(B and C) Confocal microscopy photographs of CB sections showing immunofluorescent detection of TH and endothelin receptors. Endothelin receptors A and B were both expressed in type I (arrows in B) and type II (arrowhead in C) cells. Scale bars, 50 μm.

(D and E) Immunofluorescence detection of endothelin receptor B in GFAP+ or nestin+ cells dispersed from CBs. Scale bars, 10 μm.

(F) Quantitative PCR showing a higher expression of endothelin receptor B in undifferentiated versus differentiated neurospheres (n = 3 cultures).

(G) Quantification of BrdU+ cells within CB sections of animals exposed to normoxia (Nx) or hypoxia (Hx) and treated systemically with (+B) or without bosentan (five CBs per condition).

In (F) and (G), error bars represent SEM. *$p < 0.05$ and **$p < 0.01$. See also Figures S2, S3, and Table S1.

glomus cells during exposure to hypoxia could also stimulate CB type II stem cells. This concept is fully supported by our in vivo functional experiments indicating that blockade of transmitter release with cadmium or selective genetic impairment of glomus cells results in a reduced responsiveness of the CB (activation of CB progenitor cells) to hypoxia.

The existence of synaptic-like contacts between mature glomus cells and stem cells in the CB is a structural specialization designed to optimize the general principle of the activity-dependent control of stem cell function, which appears to regulate the central neural niches. The neurogenic areas in the adult brain are innervated by projection fibers and are therefore affected by the release of several transmitters. However, the local circuitry can also control NSC function. In the SVZ, depolarization of neuroblasts induces nonsynaptic $GABA_A$ receptor currents in GFAP-positive progenitors that limit their progression through the cell cycle (Liu et al., 2005; Ge et al., 2006). Recently, it has been shown that the maintenance of stem cell quiescence in the dentate gyrus is modulated by a subset of parvalbumin-positive GABAergic interneurons, which are activated by mature granule cells (Song et al., 2012). A radical approach to stem cell control is the establishment of direct synaptic contacts between differentiated and stem cells, as has evolved in the CB niche (see Figure 7I).

ET-1 Released by Glomus Cells Activates CB Stem Cells and Organ Growth

Numerous agents released by O_2-sensitive glomus cells could mediate the activation of quiescent CB NSCs to induce organ growth. In this study, we focused on ET-1 because it is a potent proliferative agent that participates in chronic hypoxia-induced vascular wall thickening, pulmonary hypertension, and right cardiac hypertrophy (Bonvallet et al., 1994; Eddahibi et al., 1995; Oparil et al., 1995). In addition, ET-1 is known to influence the biology of neural crest progenitors during development (Hosoda et al., 1994; Shin et al., 1999; Bonano et al., 2008). Systemic administration of ET-1 activates the CB, and both ET-1 and endothelin type A receptors have been demonstrated in glomus cells (McQueen et al., 1995; Paciga et al., 1999). ET-1 released from glomus cells has been postulated to exert a paracrine/autocrine effect and to mediate CB plasticity under chronic hypoxia (Chen et al., 2002). Experiments using radiolabeled ET-1 (McQueen et al., 1995) and immunocytochemistry (Chen et al., 2002) have suggested the presence of ET-1 in glomus cells; however, the CB is rich in endothelial cells that highly express ET-1, and this could cause confounding results. Based on a combination of sorting of normal and transgenic cells with molecular biological and histological techniques, we provide unequivocal evidence that ET-1 is expressed in glomus cells in vivo

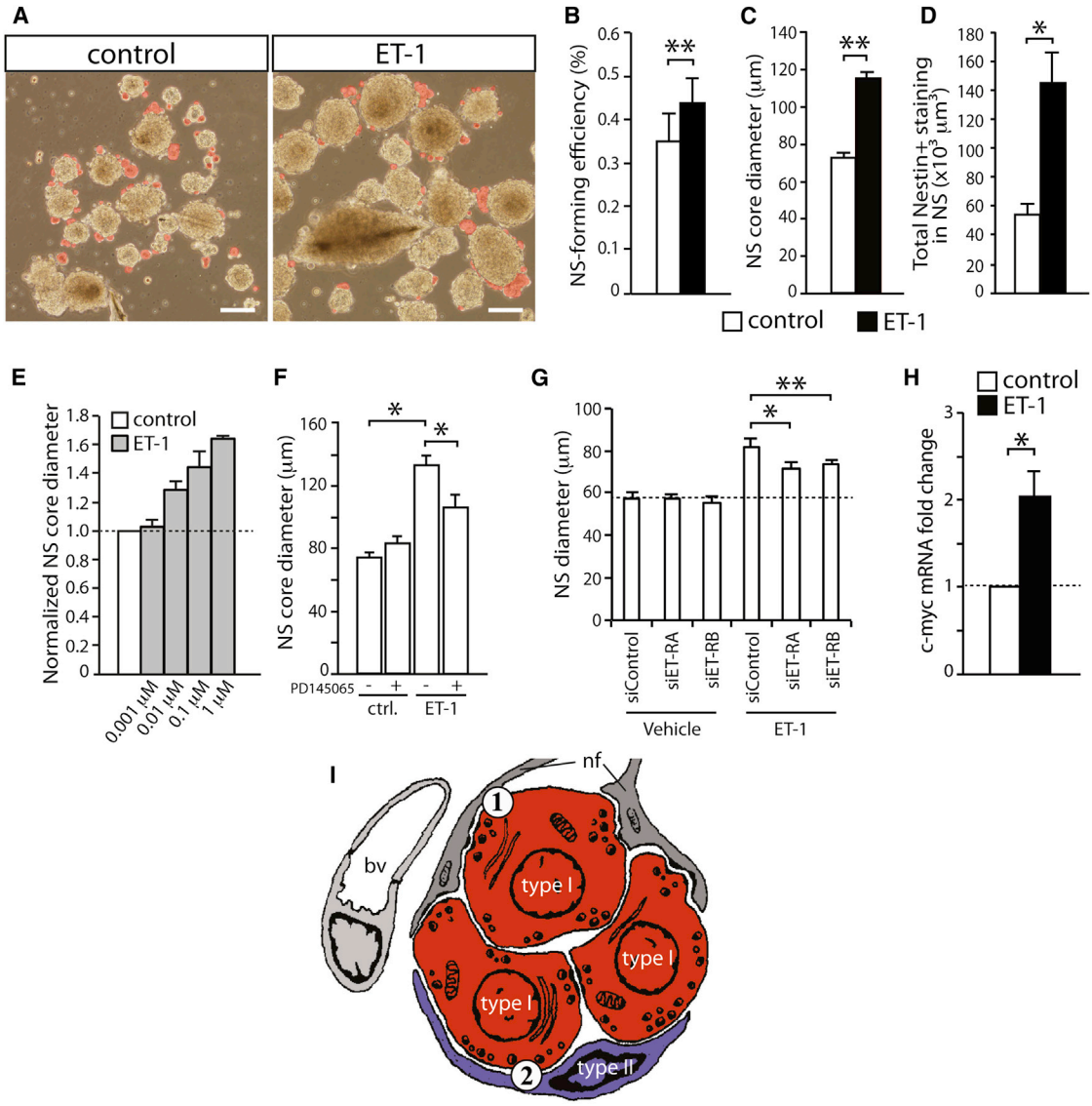

Figure 7. ET-1 Increases CB NSC Proliferation In Vitro

(A) Bright-field images of CB primary NS showing the increase in their core diameter after 10 days of culture in the presence of ET-1. Differentiating blebs are pseudocolored in red. Scale bar, 100 μm.

(B and C) Quantification of NS-forming efficiency and NS diameter from CB cultures (n = 4) treated with ET-1.

(D) Quantification of nestin+ staining within NS sections from CB cultures (n = 3) treated with ET-1.

(E) Dose-response effect of ET-1 on NS core diameter (n = 3 cultures).

(F) Measurement of NS diameter from cultures (n = 3) treated with the ET-1 receptor antagonist PD145065, which partially inhibits the effect of ET-1 (1 μM).

(G) NS diameter after downregulation of endothelin receptor expression by siRNAs (50nM) in cultures treated with (n = 5) or without (n = 4) ET-1 (0.01 μM).

(H) Increase in *c-myc* mRNA expression in NS treated with ET-1 (0.01 μM) for 10 days (n = 5 cultures).

(I) Schematic diagram illustrating the different "synaptic" communications taking place within a CB glomerulus exposed to hypoxia (bv, blood vessel; nf, sensory nerve fiber). 1, chemosensory synapse; 2, chemoproliferative synapse.

In (B–H), error bars represent SEM. *p < 0.05 and **p < 0.01. See also Figures S4, S5, and S6 and Table S1.

and in vitro. We have also shown that endothelin A receptors are expressed not only in type I cells but also in type II cells, which were excluded in previous studies. More importantly, we have found that endothelin B receptors are abundantly expressed by CB stem cells. In agreement with these observations, it has been shown that endothelin B receptors are the predominant form present in astrocytes (Koyama and Michinaga, 2012), which share the same GFAP+ cell lineage of NSCs in the brain, as well as in the CB (Pardal et al., 2007; Kriegstein and Álvarez-Buylla, 2009). ET-1 evoked proliferation of CB progenitors in vitro, and these effects were blunted by pharmacological or genetic down-regulation of ET-1 receptors. As in other tissues (Wang et al.,

1994; Shichiri et al., 1998), ET-1 induced *c-myc*, a proproliferative and antiapoptotic immediate early gene, in CB progenitors. Taken together, these data strongly suggest that ET-1 is a powerful mediator of the glomus cell-stem cell "synapse" inducing CB stem cell activation in response to low PO_2.

Studies of CB growth in chronic hypoxia have shown that, as well as indicating the differentiation of progenitor cells to newly generated glomus cells, some TH+ cells express proliferation markers (BrdU, PCNA, or Ki67) (Paciga et al., 1999; Chen et al., 2007; Pardal et al., 2007). These cells probably belong to a pool of prematured glomus cells, the abundance of which seems to vary among species. A detailed description of the proliferation of TH+ cells will be presented elsewhere. Nonetheless, the existence of close "synaptic-like" contacts between neighboring TH+ cells makes it possible that ET-1 released from glomus cells could also induce proliferation of immature TH+ cells (see Figure 7I).

Essential Role of the O_2-Sensitive Glomus Cell-Stem Cell Synapse in the Pathophysiology of Acclimatization to Hypoxia

The CB plays an important role in the reflex control of respiration in man. Individuals with bilateral CB ablation show permanent abolition of the ventilatory response to hypoxia (see Timmers et al., 2003). The CB is also essential for acclimatization to chronic hypoxia, a condition that affects millions of people who either live at or travel to high altitudes and thus are exposed to low atmospheric pressure. There are also highly prevalent human pathologic conditions, such as congestive heart failure or chronic obstructive pulmonary disease, that result in severe chronic hypoxemia due to a reduction in the O_2 exchange capacity between the air and the pulmonary capillaries. Survival under conditions of chronic hypoxia requires activation of the CB and the growth of the organ to enhance the respiratory drive necessary for sustained activation of the respiratory center (Powell et al., 1998; Joseph and Pequignot, 2009). Individuals who do not adapt well to chronic hypoxia develop neurological and cardiopulmonary dysfunctions and morbidities that can lead to death. The data presented here indicate that glomus cells are the central O_2-sensitive "presynaptic" elements that mediate CB activation in acute (chemosensory synapses, 1 in Figure 7I) and chronic (chemoproliferative synapses, 2 in Figure 7I) hypoxia. Based on these findings, the development of a functional test that evaluates CB responsiveness to hypoxia could be of value to identify hypoxia-intolerant individuals. In addition, as the neurotransmitters, cell targets, and intracellular pathways are different in the two types of O_2-sensitive synapses, the development of a selective pharmacological strategy could have potential therapeutic application.

EXPERIMENTAL PROCEDURES

Animals

Transgenic mice (see Supplemental Information), WT mice, and Wistar rats were housed and treated according to the animal care guidelines of the European Community Council (86/609/EEC). All procedures were approved by the Animal Research Committee at the University of Seville.

In Vivo Hypoxic Treatments and Drug Administration

Animals (rats and mice) were chronically exposed to a 10% or 14% O_2 environment using a hermetic isobaric chamber with O_2 and CO_2 controls and temperature and humidity monitoring (Coy Laboratory Products). To test CB growth in HIF-1$\alpha^{fl/fl}$ GFAP-cre mice, animals were exposed to hypoxia for 19 days and injected intraperitoneally with bromodeoxyuridine (BrdU) (Sigma, 50 mg/ml) at the beginning of the experiment and every 7 days. BrdU was also administered in drinking water (1 mg/ml) all the time. For the in vivo experiments with bosentan, rats (Charles River) were injected with BrdU at the beginning of the hypoxic period and divided into four groups: (1) normoxia, (2) normoxia plus bosentan, (3) chronic hypoxia, and (4) chronic hypoxia plus bosentan. Each group included the analysis of five CBs from four or five rats. Bosentan was fed to rats (100 mg/kg/day) through intragastric gavage once daily. Rats were housed in standard rodent cages with 24 hr access to pellet food and water. Bosentan treatment started 1 week before the hypoxic stimulus. Animals were maintained in the hypoxic environment for 7 days. Age-matched control rats were similarly housed in ambient air outside the chamber. Treatment with cadmium chloride ($CdCl_2$, Sigma) was performed the same way as with bosentan, except that drug administration (intraperitoneally) started only 1 day before the hypoxic period at a dose of 1 mg/kg/day. Animals were distributed in four groups (six animals per group) and were treated with $CdCl_2$ under hypoxia for 2 days, after which the CBs were dissected and dissociated. Dimethyloxalylglycine (DMOG, Frontier Scientific) was administered twice daily at a dose of 80 mg/kg by intraperitoneal injection. Animals were distributed in three groups: (1) normoxia (four CBs from three animals), (2) chronic hypoxia (five CBs from three animals), and (3) DMOG (four CBs from three animals). DMOG was prepared in saline and stored at 4°C only for a maximum of 24 hr to avoid oxidation. Rats were treated for 3 or 14 days. After treatment, the hematocrit was measured in the 14 day group. The 3 day group of rats was used to perform qRT-PCR in the brain and CB immunocytochemistry. Their brains were removed and immediately immersed in Trizol (Ambion) for subsequent RNA extraction. Carotid bifurcations were dissected and postfixed in PFA for 6 hr. In every experiment involving drug administration, control groups included the injection of the vehicle used to reconstitute the drug.

Histo- and Cytochemical Studies

For detection of TH, nestin, BrdU, Ki67, GFAP, CD31, and ET-1 receptors in tissue sections, neurospheres, and/or dispersed cells, we used standard staining procedures. Specific details are given in the Supplemental Information.

Electron Microscopy and Quantification of Dense-Core Vesicles in Type I Cells

Control and TH-SDHD mice were intracardially perfused with PBS-based fixative containing 2% PFA plus 2.5% glutaraldehyde (EMS). Carotid bifurcations were dissected and kept in the same fixative for 2 hr. The bifurcations were then postfixed in 2% osmium for 1.5 hr, rinsed, dehydrated, and embedded in Durcupan resin (Fluka). Semithin sections (1.5 μm) were cut with a diamond knife and stained with 1% toluidine blue for localization of glomeruli. Ultrathin sections (70 nm) were cut with a diamond knife, stained with lead citrate (Reynolds solution), and examined under a transmission electron microscope (FEI Tecnai G2 Spirit BioTwin) using a digital camera (Morada, Soft Imaging System, Olympus). To estimate the percentage of dense-core vesicles distributed facing the different cellular elements, we analyzed four type I cells. We counted all the vesicles that appeared in an ultrathin section. For quantification of the density of dense-core vesicles in type I cells, distributed in front of the different cell types, we analyzed several profiles of type I cells in regions in which we could clearly identify the cell types confronted.

Cell Dissociation and Neurosphere Assays

CB cell dissociation and neurosphere assays were performed as described in a previous paper form our laboratory (Pardal et al., 2007). Specific details are given in the Supplemental Information.

RT-PCR and siRNA Assays

Total RNA was extracted from intactCBs, neurospheres, or dissociated cells using a commercial kit (RNeasy MICRO kit; QIAGEN). For the extraction, 8–10 CBs, or the equivalent amount of tissue from neurospheres, was used. Specific details of the procedures used for standard and real-time quantitative PCR are given in the Supplemental Information. The oligonucleotides used are

listed in Table S1. Dispersed CB cells were transfected after 8 hr in culture with siRNA smart pools against ET-RA, ET-RB, or siRNA control smart pool (50nM; Darmacon) using lipofectamine2000 (Life Technologies-Invitrogen). Cells were allowed to form neurospheres during 7 days in the presence or absence of ET-1. This factor was added once at 64 hr after transfection. It had been tested before that a single ET-1 dose produced clear proproliferative effects on CB neurospheres. Specific mRNA downregulation was analyzed 48 hr after transfection by qPCR. It was tested that inhibition of ET-receptor mRNA expression was maintained for at least 120 hr after transfection.

Flow Cytometry

All sorts and analyses were performed as indicated before (Pardal et al., 2007). Cells dispersed from 4–6 CBs of TH-EGFP mice were sorted, and the resulting EGFP+ cells from several experiments were pooled to obtain enough RNA to perform PCR analysis. Details on animals stain and the procedures used are given in the Supplemental Information.

Statistics

Data are given as mean ± SEM. Statistical significance was estimated by paired or unpaired two sample t test. Paired t tests were used to analyze samples obtained from cell cultures and unpaired t tests were applied for the experiments involving animals. In the case of dense-core vesicle quantification, statistical significance was estimated by ANOVA and Bonferroni post hoc tests using SPSS software.

SUPPLEMENTAL INFORMATION

Supplemental Information includes Extended Experimental Procedures, six figures, and one table and can be found with this article online at http://dx.doi.org/10.1016/j.cell.2013.12.013.

ACKNOWLEDGMENTS

Research was supported by the Botín Foundation (J.L.-B.), the European Research Council (Starting Grant; R.P.), and the Spanish Ministries of Science and Innovation and Health (SAF and TERCEL programs). A.P.-L. received a predoctoral fellowship of the FPU program. We are indebted to Patricia Ortega-Sáenz, Paula García-Flores, and Francisco M. Vega for help in the experiments. We thank María José Castro and Konstantin Levitsky for technical assistance and Martine Clozel (Actelion Pharmaceuticals) for the gift of bosentan.

Received: June 5, 2013
Revised: October 7, 2013
Accepted: November 11, 2013
Published: January 16, 2014

REFERENCES

Álvarez-Buylla, A., and Lim, D.A. (2004). For the long run: maintaining germinal niches in the adult brain. Neuron *41*, 683–686.

Arias-Stella, J., and Valcarcel, J. (1976). Chief cell hyperplasia in the human carotid body at high altitudes; physiologic and pathologic significance. Hum. Pathol. *7*, 361–373.

Bishop, T., Talbot, N.P., Turner, P.J., Nicholls, L.G., Pascual, A., Hodson, E.J., Douglas, G., Fielding, J.W., Smith, T.G., Demetriades, M., et al. (2013). Carotid body hyperplasia and enhanced ventilatory responses to hypoxia in mice with heterozygous deficiency of PHD2. J. Physiol. *591*, 3565–3577.

Bonano, M., Tríbulo, C., De Calisto, J., Marchant, L., Sánchez, S.S., Mayor, R., and Aybar, M.J. (2008). A new role for the Endothelin-1/Endothelin-A receptor signaling during early neural crest specification. Dev. Biol. *323*, 114–129.

Bonvallet, S.T., Zamora, M.R., Hasunuma, K., Sato, K., Hanasato, N., Anderson, D., Sato, K., and Stelzner, T.J. (1994). BQ123, an ETA-receptor antagonist, attenuates hypoxic pulmonary hypertension in rats. Am. J. Physiol. *266*, H1327–H1331.

Buttigieg, J., and Nurse, C.A. (2004). Detection of hypoxia-evoked ATP release from chemoreceptor cells of the rat carotid body. Biochem. Biophys. Res. Commun. *322*, 82–87.

Chell, J.M., and Frisén, J. (2012). Noisy neurons keep neural stem cells quiet. Cell Stem Cell *11*, 282–284.

Chen, J., He, L., Dinger, B., Stensaas, L., and Fidone, S. (2002). Role of endothelin and endothelin A-type receptor in adaptation of the carotid body to chronic hypoxia. Am. J. Physiol. Lung Cell. Mol. Physiol. *282*, L1314–L1323.

Chen, J., He, L., Liu, X., Dinger, B., Stensaas, L., and Fidone, S. (2007). Effect of the endothelin receptor antagonist bosentan on chronic hypoxia-induced morphological and physiological changes in rat carotid body. Am. J. Physiol. Lung Cell. Mol. Physiol. *292*, L1257–L1262.

Clouthier, D.E., Hosoda, K., Richardson, J.A., Williams, S.C., Yanagisawa, H., Kuwaki, T., Kumada, M., Hammer, R.E., and Yanagisawa, M. (1998). Cranial and cardiac neural crest defects in endothelin-A receptor-deficient mice. Development *125*, 813–824.

Czyzyk-Krzeska, M.F., Bayliss, D.A., Lawson, E.E., and Millhorn, D.E. (1992). Regulation of tyrosine hydroxylase gene expression in the rat carotid body by hypoxia. J. Neurochem. *58*, 1538–1546.

Deisseroth, K., Singla, S., Toda, H., Monje, M., Palmer, T.D., and Malenka, R.C. (2004). Excitation-neurogenesis coupling in adult neural stem/progenitor cells. Neuron *42*, 535–552.

Díaz-Castro, B., Pintado, C.O., García-Flores, P., López-Barneo, J., and Piruat, J.I. (2012). Differential impairment of catecholaminergic cell maturation and survival by genetic mitochondrial complex II dysfunction. Mol. Cell. Biol. *32*, 3347–3357.

Eddahibi, S., Raffestin, B., Clozel, M., Levame, M., and Adnot, S. (1995). Protection from pulmonary hypertension with an orally active endothelin receptor antagonist in hypoxic rats. Am. J. Physiol. *268*, H828–H835.

Elton, T.S., Oparil, S., Taylor, G.R., Hicks, P.H., Yang, R.H., Jin, H., and Chen, Y.F. (1992). Normobaric hypoxia stimulates endothelin-1 gene expression in the rat. Am. J. Physiol. *263*, R1260–R1264.

Ge, S., Goh, E.L., Sailor, K.A., Kitabatake, Y., Ming, G.L., and Song, H. (2006). GABA regulates synaptic integration of newly generated neurons in the adult brain. Nature *439*, 589–593.

Heath, D., Smith, P., and Jago, R. (1982). Hyperplasia of the carotid body. J. Pathol. *138*, 115–127.

Höglinger, G.U., Rizk, P., Muriel, M.P., Duyckaerts, C., Oertel, W.H., Caille, I., and Hirsch, E.C. (2004). Dopamine depletion impairs precursor cell proliferation in Parkinson disease. Nat. Neurosci. *7*, 726–735.

Hosoda, K., Hammer, R.E., Richardson, J.A., Baynash, A.G., Cheung, J.C., Giaid, A., and Yanagisawa, M. (1994). Targeted and natural (piebald-lethal) mutations of endothelin-B receptor gene produce megacolon associated with spotted coat color in mice. Cell *79*, 1267–1276.

Joseph, V., and Pequignot, J.M. (2009). Breathing at high altitude. Cell. Mol. Life Sci. *66*, 3565–3573.

Kaelin, W.G., Jr., and Ratcliffe, P.J. (2008). Oxygen sensing by metazoans: the central role of the HIF hydroxylase pathway. Mol. Cell *30*, 393–402.

Kokovay, E., and Temple, S. (2007). Taking neural crest stem cells to new heights. Cell *131*, 234–236.

Koyama, Y., and Michinaga, S. (2012). Regulations of astrocytic functions by endothelins: roles in the pathophysiological responses of damaged brains. J. Pharmacol. Sci. *118*, 401–407.

Kriegstein, A., and Álvarez-Buylla, A. (2009). The glial nature of embryonic and adult neural stem cells. Annu. Rev. Neurosci. *32*, 149–184.

Liu, X., Wang, Q., Haydar, T.F., and Bordey, A. (2005). Nonsynaptic GABA signaling in postnatal subventricular zone controls proliferation of GFAP-expressing progenitors. Nat. Neurosci. *8*, 1179–1187.

López-Barneo, J., Pardal, R., and Ortega-Sáenz, P. (2001). Cellular mechanism of oxygen sensing. Annu. Rev. Physiol. *63*, 259–287.

McQueen, D.S., Dashwood, M.R., Cobb, V.J., Bond, S.M., Marr, C.G., and Spyer, K.M. (1995). Endothelins and rat carotid body: autoradiographic and functional pharmacological studies. J. Auton. Nerv. Syst. *53*, 115–125.

Ming, G.L., and Song, H. (2011). Adult neurogenesis in the mammalian brain: significant answers and significant questions. Neuron *70*, 687–702.

Mohyeldin, A., Garzón-Muvdi, T., and Quiñones-Hinojosa, A. (2010). Oxygen in stem cell biology: a critical component of the stem cell niche. Cell Stem Cell *7*, 150–161.

Morrison, S.J., Csete, M., Groves, A.K., Melega, W., Wold, B., and Anderson, D.J. (2000). Culture in reduced levels of oxygen promotes clonogenic sympathoadrenal differentiation by isolated neural crest stem cells. J. Neurosci. *20*, 7370–7376.

Oparil, S., Chen, S.J., Meng, Q.C., Elton, T.S., Yano, M., and Chen, Y.F. (1995). Endothelin-A receptor antagonist prevents acute hypoxia-induced pulmonary hypertension in the rat. Am. J. Physiol. *268*, L95–L100.

Ortega-Sáenz, P., Pascual, A., Piruat, J.I., and López-Barneo, J. (2007). Mechanisms of acute oxygen sensing by the carotid body: lessons from genetically modified animals. Respir. Physiol. Neurobiol. *157*, 140–147.

Ortega-Sáenz, P., Levitsky, K.L., Marcos-Almaraz, M.T., Bonilla-Henao, V., Pascual, A., and López-Barneo, J. (2010). Carotid body chemosensory responses in mice deficient of TASK channels. J. Gen. Physiol. *135*, 379–392.

Paciga, M., Vollmer, C., and Nurse, C. (1999). Role of ET-1 in hypoxia-induced mitosis of cultured rat carotid body chemoreceptors. Neuroreport *10*, 3739–3744.

Panchision, D.M. (2009). The role of oxygen in regulating neural stem cells in development and disease. J. Cell. Physiol. *220*, 562–568.

Pardal, R., Ortega-Sáenz, P., Durán, R., and López-Barneo, J. (2007). Glia-like stem cells sustain physiologic neurogenesis in the adult mammalian carotid body. Cell *131*, 364–377.

Powell, F.L., Milsom, W.K., and Mitchell, G.S. (1998). Time domains of the hypoxic ventilatory response. Respir. Physiol. *112*, 123–134.

Rubanyi, G.M., and Polokoff, M.A. (1994). Endothelins: molecular biology, biochemistry, pharmacology, physiology, and pathophysiology. Pharmacol. Rev. *46*, 325–415.

Shichiri, M., Sedivy, J.M., Marumo, F., and Hirata, Y. (1998). Endothelin-1 is a potent survival factor for c-Myc-dependent apoptosis. Mol. Endocrinol. *12*, 172–180.

Shin, M.K., Levorse, J.M., Ingram, R.S., and Tilghman, S.M. (1999). The temporal requirement for endothelin receptor-B signalling during neural crest development. Nature *402*, 496–501.

Song, J., Zhong, C., Bonaguidi, M.A., Sun, G.J., Hsu, D., Gu, Y., Meletis, K., Huang, Z.J., Ge, S., Enikolopov, G., et al. (2012). Neuronal circuitry mechanism regulating adult quiescent neural stem-cell fate decision. Nature *489*, 150–154.

Stosic, J., Mirkov, I., Belij, S., Nikolic, M., Popov, A., Kataranovski, D., and Kataranovski, M. (2010). Gender differences in pulmonary inflammation following systemic cadmium administration in rats. Biomed. Environ. Sci. *23*, 293–299.

Suda, T., Takubo, K., and Semenza, G.L. (2011). Metabolic regulation of hematopoietic stem cells in the hypoxic niche. Cell Stem Cell *9*, 298–310.

Timmers, H.J., Wieling, W., Karemaker, J.M., and Lenders, J.W. (2003). Denervation of carotid baro- and chemoreceptors in humans. J. Physiol. *553*, 3–11.

Tozuka, Y., Fukuda, S., Namba, T., Seki, T., and Hisatsune, T. (2005). GABAergic excitation promotes neuronal differentiation in adult hippocampal progenitor cells. Neuron *47*, 803–815.

Ureña, J., Fernández-Chacón, R., Benot, A.R., Álvarez de Toledo, G.A., and López-Barneo, J. (1994). Hypoxia induces voltage-dependent Ca2+ entry and quantal dopamine secretion in carotid body glomus cells. Proc. Natl. Acad. Sci. USA *91*, 10208–10211.

Wang, Y., Rose, P.M., Webb, M.L., and Dunn, M.J. (1994). Endothelins stimulate mitogen-activated protein kinase cascade through either ETA or ETB. Am. J. Physiol. *267*, C1130–C1135.

Zhao, C., Deng, W., and Gage, F.H. (2008). Mechanisms and functional implications of adult neurogenesis. Cell *132*, 645–660.